International Journal of
Molecular Sciences

MDPI

Article

Precision Medicine: Determination of Ribavirin Urinary Metabolites in Relation to Drug Adverse Effects in HCV Patients

Ottavia Giampaoli [1,2,†], Fabio Sciubba [1,2,†], Elisa Biliotti [3], Mariangela Spagnoli [4], Riccardo Calvani [5], Alberta Tomassini [1,6], Giorgio Capuani [1,6], Alfredo Miccheli [1,2,*] and Gloria Taliani [3]

1 NMR-Based Metabolomics Laboratory (NMLab), Sapienza University of Rome, 00185 Rome, Italy
2 Department of Environmental Biology, Sapienza University of Rome, 00185 Rome, Italy
3 Department of Clinical Medicine, Policlinico Umberto I, Sapienza University of Rome, 00161 Rome, Italy
4 Department of Occupational Medicine, Epidemiology and Hygiene, INAIL, Monte Porzio Catone, 00078 Rome, Italy
5 Fondazione Policlinico Universitario A. Gemelli IRCCS, 00168 Rome, Italy
6 Department of Chemistry, Sapienza University of Rome, 00185 Rome, Italy
* Correspondence: alfredo.miccheli@uniroma1.it
† These authors contributed equally to this work.

Abstract: The most commonly used antiviral treatment against hepatitis C virus is a combination of direct-acting antivirals (DAAs) and ribavirin (RBV), which leads to a shortened duration of therapy and a sustained virologic response until 98%. Nonetheless, several dose-related side effects of RBV could limit its applications. This study aims to measure the urinary concentration of RBV and its main metabolites in order to evaluate the drug metabolism ability of HCV patients and to evaluate the adverse effects, such as anemia, with respect to RBV metabolite levels. RBV and its proactive and inactive metabolites were identified and quantified in the urine of 17 HCV males with severe liver fibrosis using proton nuclear magnetic resonance (^{1}H-NMR) at the fourth week (TW4) and at the twelfth week of treatment (EOT). Four prodrug urinary metabolites, including RBV, were identified and three of them were quantified. At both the TW4 and EOT stages, six HCV patients were found to maintain high concentrations of RBV, while another six patients maintained a high level of RBV proactive metabolites, likely due to nucleosidase activity. Furthermore, a negative correlation between the reduction in hemoglobin (Hb) and proactive forms was observed, according to RBV-triphosphate accumulation causing the hemolysis. These findings represent a proof of concept regarding tailoring the drug dose in relation to the specific metabolic ability of the individual, as expected by the precision medicine approach.

Keywords: ribavirin (RBV); hepatitis C virus (HCV); severe liver fibrosis; ^{1}H-NMR; urinary metabolites

Citation: Giampaoli, O.; Sciubba, F.; Biliotti, E.; Spagnoli, M.; Calvani, R.; Tomassini, A.; Capuani, G.; Miccheli, A.; Taliani, G. Precision Medicine: Determination of Ribavirin Urinary Metabolites in Relation to Drug Adverse Effects in HCV Patients. *Int. J. Mol. Sci.* **2022**, *23*, 10043. https://doi.org/10.3390/ijms231710043

Academic Editors: Alexander Deutsch, Julia Feichtinger and Jelena Krstic

Received: 16 July 2022
Accepted: 31 August 2022
Published: 2 September 2022

1. Introduction

Chronic hepatitis C virus (HCV) infection affects over 180 million people worldwide, remaining a major cause of cirrhosis and its complications, such as hepatocellular carcinoma, liver transplantation, and liver-related death [1]. Since 2011, HCV-infected patients have usually been treated with a combination of pegylated interferon (pegIFN) and ribavirin (RBV), leading to an increased therapeutic efficacy and a sustained virological response (SVR) of up to 40% being achieved [2]. Recently, the development of direct-acting antivirals (DAAs) and their integration into HCV treatment have improved SVR rates to 100% and enabled the duration of therapy to be shortened [3,4]. Despite this, the outcomes of DAA-based therapies may be negatively impacted by comorbidities, such as advanced cirrhosis [5] or specific HCV characteristics [6,7].

Nevertheless, it has been shown that adding RBV may allow the successful re-treatment of most prior DAA failures [5]. Indeed, the efficacy of RBV is high when it

is used in combination with DAAs for both treatment-naïve and treatment-experienced patients with genotype 1 (G1) infection [8]. However, even though high rates of SVR can be achieved without RBV [9,10], the addition of RBV may be crucial for cirrhotic or treatment-experienced patients [11,12].

1-b-D-ribofuranosyl-1,2,4-triazole-3-carboxamide, known as RBV, is a guanosine nucleoside analogue with broad-spectrum antiviral activity that is a water-soluble prodrug. Once in the cell, RBV is phosphorylated by kinases into RBV-mono, di-, and triphosphate, which are pharmacologically active forms [13]. In the organism, RBV undergoes a transformation which produces the proactive metabolite 1,2,4-triazole-3-carboxamide (T-$CONH_2$) and two inactive metabolites 1-β-D-ribofuranosyl-1,2,4-triazole-3-carboxilic acid (TR-COOH) and 1,2,4-triazole-3-carboxilic acid (T-COOH); these biotransformation products are excreted in feces at a level of about 10% and in urine at a level of 72% of the dose (10% of which remains unchanged) [14,15].

RBV also enters erythrocytes through *es*-transporters and, once transformed by kinases, RBV-triphosphate accumulates excessively, since enucleated red blood cells lack dephosphorylation enzymes [16], leading to the main side effect of RBV, hemolytic anemia. It has been shown that blood accumulation and exposure to RBV at critical and stable levels may be required to achieve SVR in HCV patients infected with genotype 1b and with a high viral load [17,18]. Yet, further studies are necessary to establish the optimal steady-state RBV concentration to enable SVR to minimize the adverse events.

Genome-wide association studies have shown that human single-nucleotide polymorphisms (SNPs) are associated with RBV-induced anemia. In particular, polymorphisms near to the inosine triphosphatase (ITPA) gene locus are predictive of anemia resulting from RBV treatment [19,20]. These studies identified ITPA deficiency as a major projective factor against RBV-induced hemolytic anemia; however, the clinical utility of the SNP is limited due to the low frequency of the protective allele in the human population [13]. Indeed, two functional variants (rs1127354 and rs7270101) in the ITPA gene that cause inosine triphosphatase (ITPase) deficiency were shown to protect against RBV-induced hemolytic anemia during the early stages of treatment [21], but these variants showed strong geographical and ethnic differences in allelic frequencies [22]. However, there is still a lack of data regarding the Italian population.

In addition, oxidative damage onset related to RBV or DAAs + RBV therapy has been highlighted [23,24].

Therefore, the administration of the appropriate RBV dose is essential to manage its several adverse reactions and clinical toxicity. Few studies have been carried out aiming to adapt and validate a routine assay for the quantification of bulk, blood, and urinary RBV, in combination or not. Analytical techniques such as radioimmunoassay [25], HPLC-UV or MS detection [26–28], capillary electrophoresis [29], and the square-wave adsorptive stripping voltametric method [30] have been tested for this purpose, since no standard assay for RBV concentration determination is available for routine laboratory use. Yet, there is still a lack of data on RBV's bioavailability and excretion from large-scale clinical trials and very little information is available about RBV's main excretion products [31]. In this study, we employed for the first time the NMR-based approach to investigate the concentration of RBV and its metabolites in the urine of HCV-patients undergoing DAAs + RBV therapy. In the field of precision medicine, NMR spectroscopy has already given promising results, showing the potential to contribute to disease diagnosis [32–34]. In this regard, NMR analysis has allowed us to identify pro-active and inactive urine metabolites of RBV and to characterize the individual profiles on the basis of high and low inactivation of metabolic ability. These results could lay the foundation for the improvement of the therapeutic regime through personalized medicine, reducing RBV-related toxic effects for each individual.

2. Results

2.1. Resonance Assignment

1-β-D-ribofuranosyl-1H-1,2,4-triazole-3-carboxamide (RBV) is a nucleoside analogous to guanosine. In Figure 1, the structural formulas of RBV and its three main urinary metabolites are shown. Four metabolites were identified, including the ribosylated (TR-COOH; RBV), deribosylated (T-$CONH_2$; T-COOH), amidic (T-$CONH_2$; RBV), and acid forms (TR-COOH; T-COOH).

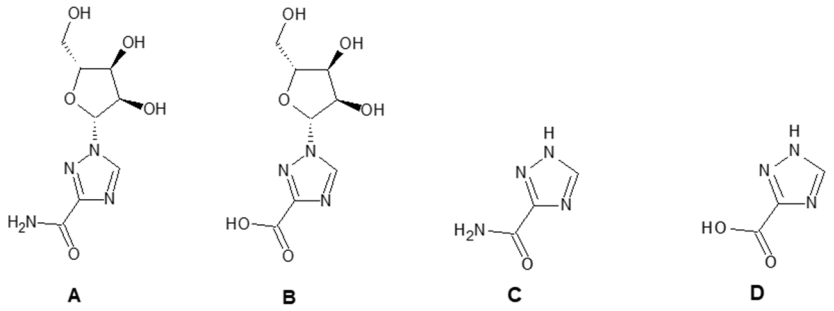

Figure 1. RBV and its metabolites. **A**: RBV; **B**: TR-COOH; **C**: T-$CONH_2$; **D**: T-COOH.

In order to assess the assignment of RBV and its metabolites, two zones of the whole NMR spectrum have been taken into account:

(1) Spectral region between 5.97 and 6.10 ppm (resonances of ribosyl moiety);
(2) Aromatic region between 8.50 and 8.80 ppm (resonances of triazole moiety).

The assignments of RBV and its metabolites in the urine samples of patients under therapy are shown in Table 1.

Table 1. ^{1}H-NMR assignment of RBV and its metabolites in urine. The integrated resonances for quantitative analysis are reported in bold.

Name	Structure	Assignment	δ (ppm) ^{1}H	Multiplicity
RBV	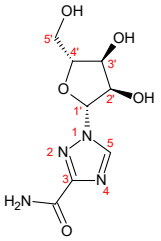	5′-CH_2	3.80–3.90	m
		4′-CH	4.50	m
		3′-CH	4.24	m
		2′-CH	4.25	m
		1′-CH	6.07	d
		5-CH	**8.76**	**s**
TR-COOH	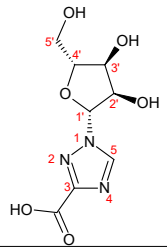	5′-CH_2	3.80–3.90	m
		4′-CH	4.50	m
		3′-CH	4.24	m
		2′-CH	4.25	m
		1′-CH	6.01	d
		5-CH	**8.65**	**s**
T-$CONH_2$	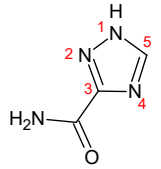	**5-CH**	**8.53**	**s**

Concerning the spectral region between 5.97 and 6.10 ppm (Figure 2), it was possible to observe two different ribosyl moieties, whose resonances were univocally assigned on the basis of TOCSY experiments (Figure 3).

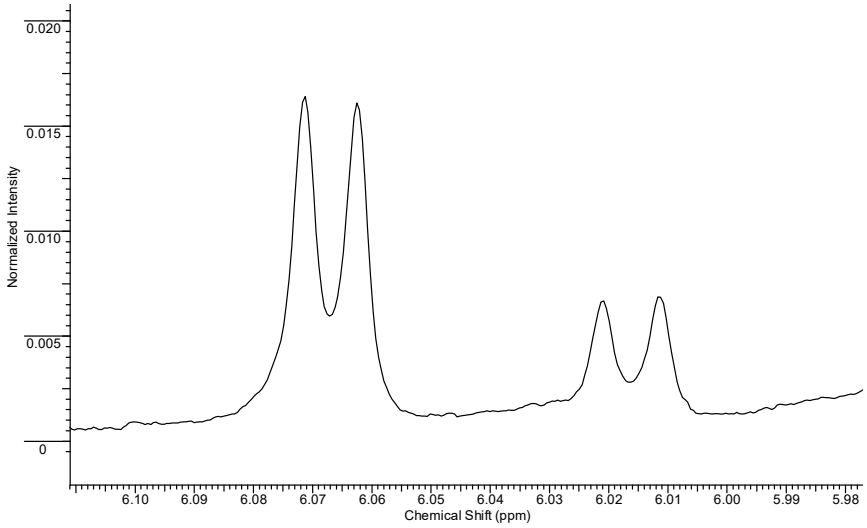

Figure 2. Spectral region between 5.97 and 6.10 ppm.

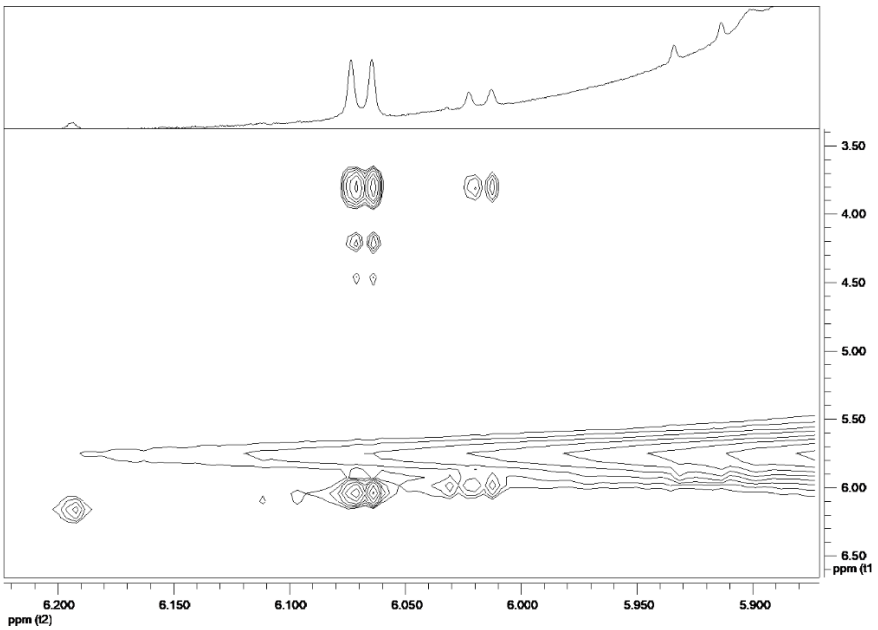

Figure 3. TOCSY spectrum showing correlation pattern of ribosylic moieties.

With regard to the triazolic ring (Figure 4), we observed three singlets in the spectral region between 8.50 and 8.80 ppm.

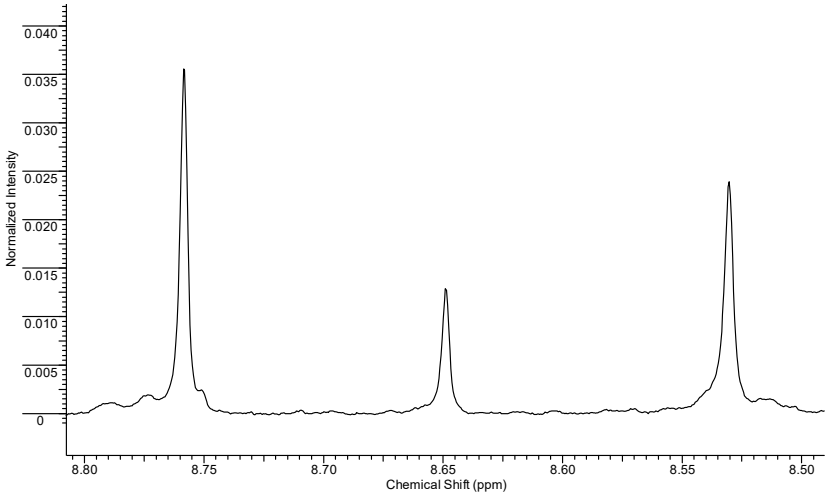

Figure 4. Spectral region between 8.50 and 8.80 ppm.

On the basis of literature data [35] and HSQC experiments (Figure 4), it was possible to univocally identify the RBV resonances, with the H-5 proton resonating at 8.76 ppm and the corresponding H-1′ of the ribosyl moiety resonating at 6.07 ppm.

Concerning the ribosyl moiety whose anomeric proton resonates at 6.01 ppm, on the basis of the relative integrals between this proton and triazolic ring one, it is possible to univocally assign the TR-COOH H-5 to the resonance at 8.65 ppm.

The singlet resonating at 8.53 ppm can be attributed to T-$CONH_2$ on the basis of the HSQC experiment (Figure 5), since the corresponding carbon resonance (150 ppm) is closer to the one of RBV (150 ppm) than that of TR-COOH, which resonates at 149 ppm. The similarity in the carbon chemical shift indicates that the resonance structures of the two rings are rather similar and this is only possible if the carboxyl group is substituted with an amidic group. The absence of the ribosyl moiety mainly influences the proton chemical shift, which is 0.23 ppm lower compared to RBV.

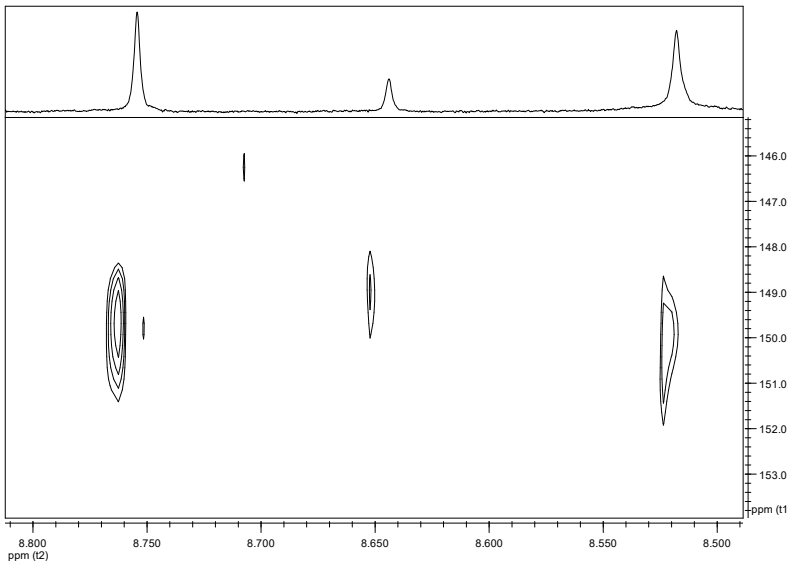

Figure 5. HSQC spectrum showing the resonances of triazolic H-5 for the RBV and its metabolites.

We then spiked a control urine sample with different concentrations of T-COOH, T-$CONH_2$, and TR-COOH (Figure 6), thus also confirming the obtained results on the basis of the ratio of integrals. RBV was not added to the urine sample, since it has already been reported elsewhere [35].

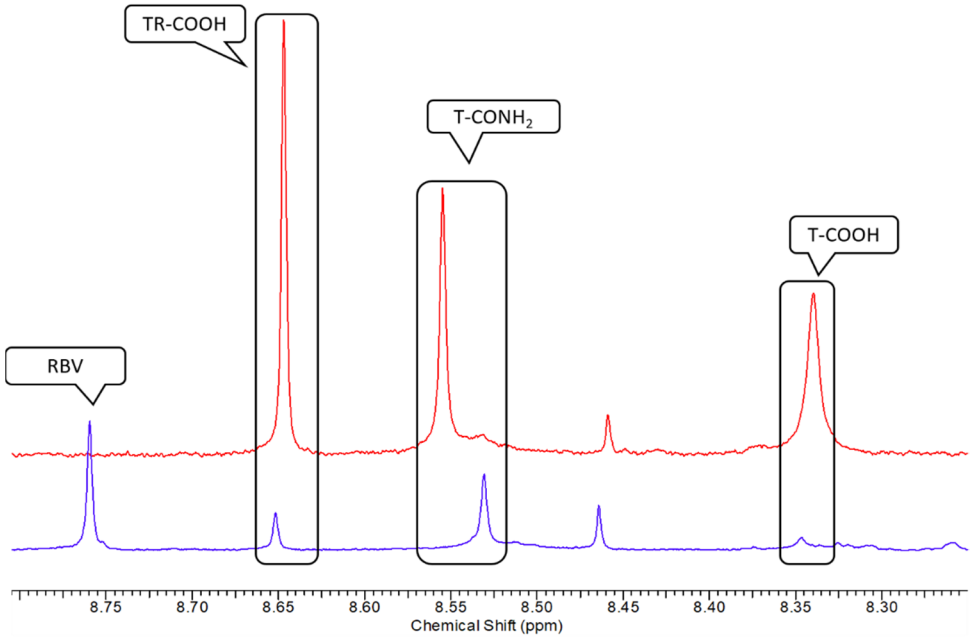

Figure 6. From the bottom to the top, ^{1}H NMR urine aromatic region of an HCV patient at TW4 stage (blue) and a control spiked with TR-COOH, T-CONH$_2$, and T-COOH (red). Small variations in chemical shift can be attributed to the different ionic strengths and the small variation in pH in the urine sample.

As a validation of this assignment, we recorded the reference spectra of each molecule (Supplementary Figure S1).

2.2. Quantitative Analysis

In order to assess the drug metabolism changes during therapy, proactive and inactive forms of RBV were quantified.

The quantitative analysis was carried out starting from the integration of TR-COOH, RBV, and T-CONH$_2$.

The T-COOH metabolite was identified in all the examined samples; however, its quantification was not possible due to the low intensity of the signal and the high overlapping of resonances. The concentrations of each metabolite, expressed as µmol/mmol of creatinine, are reported in Supplementary Table S4 for treatment week four (TW4) and treatment week twelve (end of treatment, EOT).

Based on the relative amounts of urinary RBV and T-CONH$_2$, 12 out of 17 patients were recognized to show the same urinary excretion at both TW4 and EOT, having ratios of RBV/T-CONH$_2$ higher than 1 (phenotype 1, patient IDs 09, 12, 16, 20, 47, 48) and lower than 1 (phenotype 2, patient IDs 14, 19, 40, 42, 43, 50).

Each patient enrolled in this study experienced a reduction in Hb levels from baseline (T0) to TW4 and EOT, separately (Supplementary Table S3).

To better investigate the phenomenon, Pearson correlation analysis was performed for TW4 and EOT separately, excluding patient ID 43, taking into account the amounts of RBV, its metabolites, and the delta variation in Hb with respect to the baseline (Table 2).

A negative correlation between the Hb fold ratio (Hb values at TW4 or EOT with respect to baseline) and the $\frac{RBV}{T-CONH_2}$ ratio was observed at both the TW4 and EOT stages, even though the latter correlation did not achieve the statistical significance.

Table 2. Pearson correlation values with the corresponding *p* value for TW4 and EOT patients (*n* = 16). Fold ratio of Hb was determined with respect to the baseline.

		TW4	EOT
		$\frac{RBV}{T-CONH_2}$	$\frac{RBV}{T-CONH_2}$
TW4	Fold Ratio Hb	**−0.520** **0.039**	
EOT	Fold Ratio Hb		**−0.326** **NS**

In addition, a targeted metabolomic analysis was carried out considering the significant metabolites related to DAA treatment and severe liver fibrosis effects, according to a previously published work [24]. In particular, pseudouridine (PSI), hypoxanthine (Hyp), methylguanidine (MG), dimethylamine (DMA), tyrosine (Tyr), and glutamine (Gln) were associated with the severe liver fibrosis; 1-methylnicotinamide (1-MNA) and 3-hydroxy-3-methylbutyrate (3-HMB) were associated with the HCV clearance; and 3-hydroxyisobutyrate (3-HIB), 2,3-dihydroxy-2-methylbutyrate (2,3-DH-2-MB), and glycine (Gly) were associated with the DAA treatment effect. The NMR assignments of these metabolites are reported elsewhere [24], while the quantitative analysis is reported in Supplementary Table S4.

In order to investigate if the different urinary excretion of proactive and inactive forms could be associated with the abovementioned metabolites, Spearman correlation analysis was performed separately on TW4 and EOT datasets.

Regarding TW4 patients, TR-COOH was positively correlated with PSI and with RBV (Table 3).

Table 3. Significant *p* values reported according to Spearman correlations for TW4 patients (*n* = 17).

	Correlation *p* Values		
	T-$CONH_2$	**TR-COOH**	**RBV**
PSI	NS	0.036	NS
TR-COOH	NS	-	<0.01

In EOT patients, RBV was positively correlated with T-$CONH_2$ and, interestingly, together with all its metabolites it positively correlated with Hyp (Table 4).

Table 4. Significant *p* values reported according to Spearman correlations for EOT patients (*n* = 17).

	Correlation *p* Values		
	T-$CONH_2$	**TR-COOH**	**RBV**
Hyp	0.038	<0.01	0.011
T-$CONH_2$	-	<0.01	0.0164
TR-COOH	-	-	<0.01

3. Discussion

Patients with chronic HCV infections can experience adverse reactions to DAA therapy. The severity of these adverse effects is dose-dependent.

As is well known, the major dose-related toxicity of RBV is reversible hemolytic anemia, which occurs in up to one-third of patients and is due to the accumulation of RBV-triphosphate within erythrocytes. Since the RBV anemia dependent is fully reversible, the dosage of RBV is then reduced as a function of the hemoglobin (Hb) levels [36]. This

is a unique biomarker useful for regulating the RBV dose during treatment; however, it cannot be used for patients with cardiomyopathy disease [37].

The interconversion of the forms of RBV is linked to the activity of three key enzymes: adenosine deaminase, nucleosidases, and adenosine kinases (Figure 7). Interestingly, these enzymes are all present within the cells, while adenosine deaminase is also present in the blood stream [38,39].

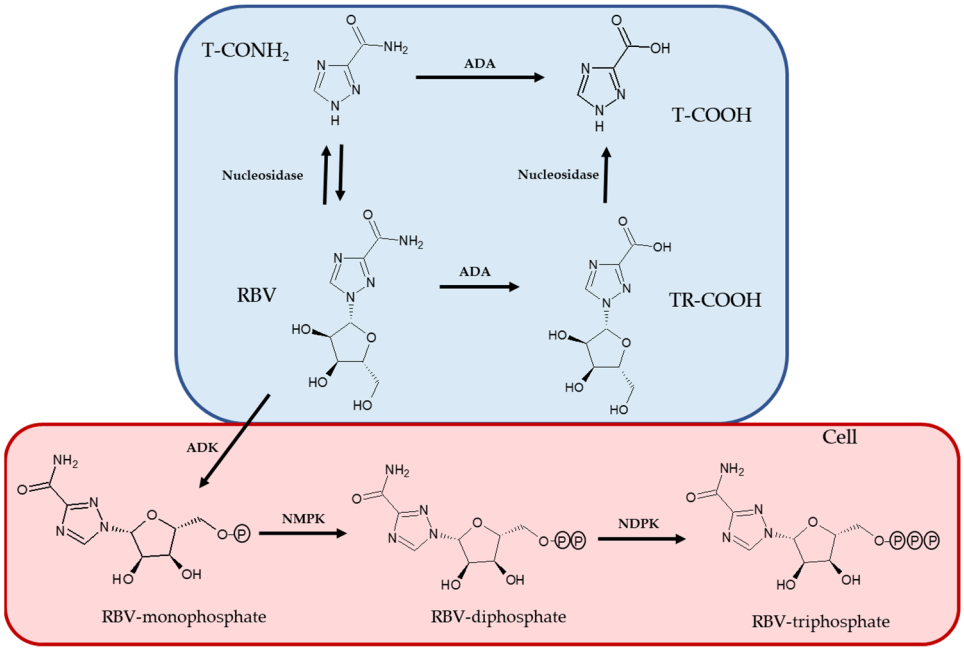

Figure 7. RBV metabolic pathway. Blue: extracellular compartment; red: intracellular compartment. ADA: adenosine deaminase; ADK: adenosine kinase; NMPK: nucleoside monophosphate kinase; NDPK: nucleoside diphosphate kinase.

Our results showed that the reduction in Hb correlated with higher values of the RBV/T-$CONH_2$ metabolite ratio, mainly at the TW4 stage (Table 2). The negative correlation observed at TW4 and EOT was in agreement with the absence of specific enzymes for RBV-triphosphate dephosphorylation in erythrocytes, leading to the accumulation of active molecules and, therefore, causing hemolysis. From our results, the relationship between the proactive metabolites remained unchanged throughout the therapy for 12 out of 17 patients, strongly suggesting the importance of quantifying the concentration of proactive metabolites excreted to allow for an individual optimization of the RBV dosage before a severe reduction in Hb levels. The difference in the phenotypes observed could be associated with the nucleosidase activity, since this enzyme regulates the equilibrium between RBV and T-$CONH_2$ (Figure 7) [14].

Another interesting aspect of this study was the investigation of the relationship between the changes in RBV metabolite levels and the urinary metabolic biomarkers associated with hepatic fibrosis and the side effects of antiviral treatment.

A positive correlation between urinary TR-COOH levels and PSI was observed at the TW4 stage. PSI is a post-transcriptionally modified nucleoside derived from mRNA catabolism. Since RBV is preferentially active in RNA-related metabolism [40], the observed correlation between these urinary metabolites was in agreement with a higher mRNA turnover.

On the contrary, Hyp is the only metabolite that correlates positively with all metabolites of RBV at the EOT stage.

Hyp is an intermediate involved in the purine metabolic pathway and has been found to be associated with oxidative damage in liver fibrosis [24,41]. One of RBV's proposed mechanisms of action affects purine metabolism, since RBV is a competitive

inhibitor of the inosine monophosphate dehydrogenase (IMPDH) enzyme, which converts inosine-5-monophosphate into xanthine-5-monophosphate, leading to a depletion of guanosine-triphosphate (GTP) [13,16]. The positive correlation of Hyp levels with all forms of RBV metabolites is in agreement with the RBV molecular mechanism of action on purine metabolism, increasing the Hyp levels in patients with altered purine metabolism depending on hepatic fibrosis [24].

In conclusion, although this study has some limitations due to the small number and gender exclusivity of enrolled patients, it represents an important example of personalized management of pharmacological treatment to prevent undesired effects.

4. Materials and Methods

4.1. Study Population

From a population cohort of 130 HCV patients, 17 male patients with HCV severe liver fibrosis who had received DAAs + RBV therapy were selected for the analysis to minimize the interindividual variability. Each patient was considered at two time points: the fourth week of treatment (TW4) and the twelfth week of treatment (end of treatment, EOT).

The exclusion criteria were HIV co-infection, female sex, genotype other than 1, and an estimated glomerular filtration rate eGFR $\leq$ 60 mL/MIN/1.73 m^2. The anthropometric and clinical data and the therapies of patients involved in this study are reported in Supplementary Tables S1 and S2. Sustained virologic response (SVR), defined as serum HCV-RNA undetectability 12 weeks after EOT, was achieved in all patients.

The study protocol conformed to the ethical guidelines of the 1975 Declaration of Helsinki and was approved by the Institutional Review Board. All patients provided their written informed consent to participate in the study.

4.2. Chemicals

The standards of T-$CONH_2$, T-COOH, and TR-COOH were provided by Toronto Research Chemicals (20 Martin Ross Avenue, Toronto, ON, Canada). Deuterium oxide (D_2O, deuteration degree of 99.95%) was provided by Sigma-Aldrich (ON, Canada). 3-trymethylsilyl propionic 2,2,3,3-d_4 acid, sodium salt (TSP, deuteration degree of 98%), was purchased from Sigma-Aldrich (Saint Louis, MO, USA).

4.3. Sample Preparation

For each urine sample, 2 mL aliquots were collected and centrifuged for 15 min at 3000× *g* in order to precipitate any particulate matter using an Itettich Zentrifugen (Tuttlingen, Germany). A total of 120 µL of a 10× concentrated solution of TSP used as an internal standard in phosphate buffer–D_2O was added to 1200 µL of the centrifuged sample. The pH of urine was measured and adjusted in the pH range 6.95–7.05 by adding NaOH or HCl 0.1 N in order to eliminate changes in chemical shifts. Finally, 600 µL of each sample was stored at −80 °C. For the NMR analysis, the materials used were D_2O (ISOTEC Stable Isotopes) with an isotopic purity of 99.96% and TSP (used as internal standard) with an isotopic purity of 98%. Both of them were purchased from Sigma Aldrich (St. Louis, MO, USA).

4.4. NMR Analysis

All spectra were recorded at 298 K on a Bruker AVANCE^{TM} 400 (Bruker Spectrospin Company, Milan, Italy) spectrometer equipped with a Bruker multinuclear z-gradient 5 mm probehead. Spectra were recorded operating at the proton frequency of 400.13 MHz and at the carbon frequency of 100.16 MHz, corresponding to 9.4 T. The experiments were carried out using a 90° pulse for 15 µs, employing the 2 s length presat pulse sequence in the instrumental routine.

^{1}H-NMR spectra were acquired by collecting 64 scans for each spectrum and 64 k data points for an acquisition time of 5.45 s. The recycle delay was set to achieve a 13 s total acquisition time to avoid relaxation effects, as reported elsewhere [42]. TOCSY

experiments were conducted with a spectral width of 6000 Hz in both dimensions, a data matrix of 8192 × 256 points, a mixing time of 110 ms, and a relaxation delay of 2 s. HSQC experiments were performed with spectral widths of 6000 and 25,500 Hz for the proton and carbon, respectively; a data matrix of 8192 × 256 points; and a recycle delay of 2 s. HMBC spectra were acquired with a spectral width of 6000 and 25,500 Hz for the proton and carbon, respectively; a data matrix of 8192 × 256 points; long-range constants J_{C-H} of 4, 8, and 12 Hz; and a recycle delay of 2 s.

Monodimensional NMR spectra were processed and quantified using the ACD Lab 1D-NMR Manager ver. 12.0 software (Advanced Chemistry Development, Inc., Toronto, ON, Canada), whereas 2D-NMR spectra were processed using MestreC and ACD/Labs. The NMR spectra were manually phased, baseline-corrected, and referenced to the chemical shift of the TSP methyl resonance at δ 0.00. The quantification of metabolites was performed by comparing the integrals to the internal standard TSP integral. Metabolite's concentrations were expressed as μmol/mmol creatinine, using the creatinine methylene group signal at 4.05 ppm as a normalizing factor.

4.5. Statistical Analysis

Pearson and Spearman correlations were employed for normal or non-normal distributions, respectively, to correlate the urinary levels of drug metabolites with those of Hb and targeted analysis metabolites. Both the analyses were carried out using Sigma plot 14 (Systat Software, Palo Alto, CA, USA). A *p*-value of 0.05 was considered as the threshold for statistical significance.

Supplementary Materials: The following are available online at https://www.mdpi.com/article/10.3390/ijms231710043/s1.

Author Contributions: Conceptualization, A.M. and G.T.; methodology, A.M., O.G., F.S., E.B. and R.C.; software, O.G. and F.S.; formal analysis, O.G., E.B., F.S., G.C. and A.T.; investigation, A.M., O.G., F.S., E.B. and G.T.; data curation, O.G., F.S., E.B. and M.S.; writing—original draft preparation, A.M., O.G. and F.S; writing—review and editing, A.M., O.G., F.S., M.S. and R.C.; visualization, A.M., O.G., F.S., M.S. and R.C.; supervision, A.M. and G.T.; project administration, G.T.; funding acquisition, G.T., O.G. and F.S. contributed equally to this study. All authors have read and agreed to the published version of the manuscript.

Funding: This research was funded by Sapienza University of Rome (Research Project 2017).

Institutional Review Board Statement: The study was conducted according to the guidelines of the Declaration of Helsinki, and approved by the Institutional Review Board (or Ethics Committee) of Sapienza Università di Roma (Sapienza Research Project 2017, n° 224C, 20 November 2017).

Informed Consent Statement: Informed consent was obtained from all subjects involved in the study.

Data Availability Statement: Data are available as Supplementary Materials.

Conflicts of Interest: The authors declare no conflict of interest.

References

1. Blach, S.; Zeuzem, S.; Manns, M.; Altraif, I.; Duberg, A.-S.; Muljono, D.H.; Waked, I.; Alavian, S.M.; Lee, M.-H.; Negro, F.; et al. Global prevalence and genotype distribution of hepatitis C virus infection in 2015: A modelling study. *Lancet Gastroenterol. Hepatol.* **2016**, *2*, 161–176. [CrossRef]
2. De Clercq, E. Current race in the development of DAAs (direct-acting antivirals) against HCV. *Biochem. Pharmacol.* **2014**, *89*, 441–452. [CrossRef]
3. Ghany, M.G.; Nelson, D.R.; Strader, D.B.; Thomas, D.L.; Seeff, L.B. An update on treatment of genotype 1 chronic hepatitis C virus infection: 2011 practice guideline by the American Association for the Study of Liver Diseases. *Hepatology* **2011**, *54*, 1433–1444. [CrossRef]
4. Lu, M.; Wu, K.; Li, J.; Moorman, A.C.; Spradling, P.R.; Teshale, E.H.; Boscarino, J.A.; Daida, Y.G.; Schmidt, M.A.; Rupp, L.B.; et al. Adjuvant ribavirin and longer direct-acting antiviral treatment duration improve sustained virological response among hepatitis C patients at risk of treatment failure. *J. Viral Hepat.* **2019**, *26*, 1210–1217. [CrossRef]

5. Benítez-Gutiérrez, L.; Barreiro, P.; Labarga, P.; De Mendoza, C.; Montero, J.V.F.; Arias, A.; Peña, J.M.; Soriano, V. Prevention and management of treatment failure to new oral hepatitis C drugs. *Expert Opin. Pharmacother.* **2016**, *17*, 1215–1223. [CrossRef]
6. Di Maio, V.C.; Barbaliscia, S.; Teti, E.; Fiorentino, G.; Milana, M.; Paolucci, S.; Pollicino, T.; Morsica, G.; Starace, M.; Bruzzone, B.; et al. Resistance analysis and treatment outcomes in hepatitis C virus genotype 3-infected patients within the Italian network VIRONET-C. *Liver Int.* **2021**, *41*, 1802–1814. [CrossRef]
7. Di Stefano, M.; Faleo, G.; Mohamed, A.M.F.; Morella, S.; Bruno, S.R.; Tundo, P.; Fiore, J.R.; Santantonio, T.A. Resistance Associated Mutations in HCV Patients Failing DAA Treatment. *New Microbiol.* **2021**, *44*, 12–18.
8. Mathur, P.; Kottilil, S.; Wilson, E. Use of Ribavirin for Hepatitis C Treatment in the Modern Direct-acting Antiviral Era. *J. Clin. Transl. Hepatol.* **2018**, *6*, 431. [CrossRef]
9. Charlton, M.; Everson, G.T.; Flamm, S.L.; Kumar, P.; Landis, C.; Brown, R.S.; Fried, M.W.; Terrault, N.A.; O'Leary, J.G.; Vargas, H.E.; et al. Ledipasvir and Sofosbuvir Plus Ribavirin for Treatment of HCV Infection in Patients with Advanced Liver Disease. *Gastroenterology* **2015**, *149*, 649–659. [CrossRef]
10. Saxena, V.; Khungar, V.; Verna, E.C.; Levitsky, J.; Brown, R.S., Jr.; Hassan, M.A.; Sulkowski, M.S.; O'Leary, J.G.; Koraishy, F.; Galati, J.S.; et al. Safety and efficacy of current direct-acting antiviral regimens in kidney and liver transplant recipients with hepatitis C: Results from the HCV-TARGET study. *Hepatology* **2017**, *66*, 1090–1101. [CrossRef]
11. Lionetti, R.; Piccolo, P.; Lenci, I.; Siciliano, M.; Visco-Comandini, U.; De Santis, A.; Pompili, M.; Milana, M.; Taibi, C.; Dell'Isola, S.; et al. Daclatasvir, sofosbuvir with or without ribavirin for 24 weeks in hepatitis C genotype 3 cirrhosis: A real-life study. *Ann. Hepatol.* **2019**, *18*, 434–438. [CrossRef]
12. Kwo, P.; Gane, E.J.; Peng, C.-Y.; Pearlman, B.; Vierling, J.M.; Serfaty, L.; Buti, M.; Shafran, S.; Stryszak, P.; Lin, L.; et al. Effectiveness of Elbasvir and Grazoprevir Combination, With or Without Ribavirin, for Treatment-Experienced Patients with Chronic Hepatitis C Infection. *Gastroenterology* **2017**, *152*, 164–175.e4. [CrossRef]
13. Thomas, E.; Ghany, M.G.; Liang, T.J. The Application and Mechanism of Action of Ribavirin in Therapy of Hepatitis C. *Antivir. Chem. Chemother.* **2012**, *23*, 1–12. [CrossRef]
14. Miller, J.P.; Kigwana, L.J.; Streeter, D.G.; Robins, R.K.; Simon, L.N.; Roboz, J. The Relationship between the Metabolism of Ribavirin and Its Proposed Mechanism of Action. *Ann. N. Y. Acad. Sci.* **1977**, *284*, 211–229. [CrossRef]
15. Lin, C.-C.; Yeh, L.-T.; Luu, T.; Lourenco, D.; Lau, J.Y.N. Pharmacokinetics and Metabolism of [14C] Ribavirin in Rats and Cynomolgus Monkeys. *Antimicrob. Agents Chemother.* **2003**, *47*, 1395–1398. [CrossRef]
16. Dixit, N.M.; Perelson, A.S. The metabolism, pharmacokinetics and mechanisms of antiviral activity of ribavirin against hepatitis C virus. *Experientia* **2006**, *63*, 832–842. [CrossRef]
17. Tsubota, A.; Hirose, Y.; Izumi, N.; Kumada, H. Pharmacokinetics of ribavirin in combined interferon-alpha 2b and ribavirin therapy for chronic hepatitis C virus infection. *Br. J. Clin. Pharmacol.* **2003**, *55*, 360–367. [CrossRef]
18. Tsubota, A.; Arase, Y.; Suzuki, F.; Suzuki, Y.; Akuta, N.; Hosaka, T.; Someya, T.; Kobayashi, M.; Saitoh, S.; Ikeda, K.; et al. High-dose interferon alpha-2b induction therapy in combination with ribavirin for Japanese patients infected with hepatitis C virus genotype 1b with a high baseline viral load. *J. Gastroenterol.* **2004**, *39*, 155–161. [CrossRef]
19. Fellay, J.; Thompson, A.J.; Ge, D.; Gumbs, C.E.; Urban, T.J.; Shianna, K.V.; Little, L.D.; Qiu, P.; Bertelsen, A.H.; Watson, M.; et al. ITPA gene variants protect against anaemia in patients treated for chronic hepatitis C. *Nature* **2010**, *464*, 405–408. [CrossRef]
20. Miyamura, T.; Kanda, T.; Nakamoto, S.; Wu, S.; Jiang, X.; Arai, M.; Fujiwara, K.; Imazeki, F.; Yokosuka, O. Roles of ITPA and IL28B Genotypes in Chronic Hepatitis C Patients Treated with Peginterferon Plus Ribavirin. *Viruses* **2012**, *4*, 1264–1278. [CrossRef]
21. Thompson, A.J.; Fellay, J.; Patel, K.; Tillmann, H.L.; Naggie, S.; Ge, D.; Urban, T.J.; Shianna, K.V.; Muir, A.J.; Fried, M.W.; et al. Variants in the ITPA Gene Protect Against Ribavirin-Induced Hemolytic Anemia and Decrease the Need for Ribavirin Dose Reduction. *Gastroenterology* **2010**, *139*, 1181–1189.e2. [CrossRef]
22. D'Avolio, A.; Cusato, J.; De Nicolò, A.; Allegra, S.; Di Perri, G. Pharmacogenetics of ribavirin-induced anemia in HCV patients. *Pharmacogenomics* **2016**, *17*, 925–941. [CrossRef]
23. De Franceschi, L.; Fattovich, G.; Turrini, F.; Ayi, K.; Brugnara, C.; Manzato, F.; Noventa, F.; Stanzial, A.M.; Solero, P.; Corrocher, R. Hemolytic anemia induced by ribavirin therapy in patients with chronic hepatitis C virus infection: Role of membrane oxidative damage. *Hepatology* **2000**, *31*, 997–1004. [CrossRef]
24. Biliotti, E.; Giampaoli, O.; Sciubba, F.; Marini, F.; Tomassini, A.; Palazzo, D.; Capuani, G.; Esvan, R.; Spaziante, M.; Taliani, G.; et al. Urinary metabolomics of HCV patients with severe liver fibrosis before and during the sustained virologic response achieved by direct acting antiviral treatment. *Biomed. Pharmacother.* **2021**, *143*, 112217. [CrossRef]
25. Granich, G.G.; Krogstad, D.J.; Connor, J.D.; Desrochers, K.L.; Sherwood, C. High-performance liquid chromatography (HPLC) assay for ribavirin and comparison of the HPLC assay with radioimmunoassay. *Antimicrob. Agents Chemother.* **1989**, *33*, 311–315. [CrossRef]
26. A Youssef, A.; Magdy, N.; A Hussein, L.; El-Kosasy, A.M. Validated RP-HPLC Method for Simultaneous Determination of Ribavirin, Sofosbuvir and Daclatasvir in Human Plasma: A Treatment Protocol Administered to HCV Patients in Egypt. *J. Chromatogr. Sci.* **2019**, *57*, 636–643. [CrossRef]
27. Aouri, M.; Moradpour, D.; Cavassini, M.; Mercier, T.; Buclin, T.; Csajka, C.; Telenti, A.; Rauch, A.; Decosterd, L.A. Multiplex Liquid Chromatography-Tandem Mass Spectrometry Assay for Simultaneous Therapeutic Drug Monitoring of Ribavirin, Boceprevir, and Telaprevir. *Antimicrob. Agents Chemother.* **2013**, *57*, 3147–3158. [CrossRef]

28. Homma, M.; Jayewardene, A.L.; Gambertoglio, J.; Aweeka, F. High-Performance Liquid Chromatographic Determination of Ribavirin in Whole Blood to Assess Disposition in Erythrocytes. *Antimicrob. Agents Chemother.* **1999**, *43*, 2716–2719. [CrossRef]
29. Breadmore, M.C.; Theurillat, R.; Thormann, W. Determination of ribavirin in human serum and plasma by capillary electrophoresis. *Electrophoresis* **2004**, *25*, 1615–1622. [CrossRef]
30. Abdel Gaber, A.A.; Ahmed, S.A.; Abdel Rahim, A.M. Cathodic adsorptive stripping voltammetric determination of Ribavirin in pharmaceutical dosage form, urine and serum. *Arab. J. Chem.* **2017**, *10*, S2175–S2181. [CrossRef]
31. de Kanter, C.T.M.M.; Drenth, J.P.H.; Arends, J.E.; Reesink, H.W.; van der Valk, M.; de Knegt, R.J.; Burger, D.M. Viral Hepatitis C Therapy: Pharmacokinetic and Pharmacodynamic Considerations. *Clin. Pharmacokinet.* **2014**, *53*, 409–427. [CrossRef]
32. Zhang, A.-H.; Sun, H.; Qiu, S.; Wang, X.-J. NMR-based metabolomics coupled with pattern recognition methods in biomarker discovery and disease diagnosis. *Magn. Reson. Chem.* **2013**, *51*, 549–556. [CrossRef]
33. Silva, R.A.; Pereira, T.C.; Souza, A.R.; Ribeiro, P.R. 1H NMR-based metabolite profiling for biomarker identification. *Clin. Chim. Acta* **2019**, *502*, 269–279. [CrossRef]
34. Everett, J.R. NMR-based pharmacometabonomics: A new paradigm for personalised or precision medicine. *Prog. Nucl. Magn. Reson. Spectrosc.* **2017**, *102–103*, 1–14. [CrossRef]
35. Mandal, R.; Ta, A.; Sinha, R.; Theeya, N.; Ghosh, A.; Tasneem, M.; Bhunia, A.; Koley, H.; Das, S. Ribavirin suppresses bacterial virulence by targeting LysR-type transcriptional regulators. *Sci. Rep.* **2016**, *6*, 39454. [CrossRef]
36. Poniachik, J. Management of adverse reactions to chronic hepatitis C treatment. *Ann. Hepatol.* **2006**, *5*, S67–S68. [CrossRef]
37. Durante-Mangoni, E.; Iossa, D.; Pinto, D.; De Vincentiis, L.; Ragone, E.; Utili, R. Safety and efficacy of peginterferon alpha plus ribavirin in patients with chronic hepatitis C and coexisting heart disease. *Dig. Liver Dis.* **2011**, *43*, 411–415. [CrossRef]
38. Iwaki-Egawa, S.; Yamamoto, T.; Watanabe, Y. Human plasma adenosine deaminase 2 is secreted by activated monocytes. *Biol. Chem.* **2006**, *387*, 319–321. [CrossRef]
39. Schrader, W.P.; West, C. Localization of adenosine deaminase and adenosine deaminase complexing protein in rabbit heart. Implications for adenosine metabolism. *Circ. Res.* **1990**, *66*, 754–762. [CrossRef]
40. Crotty, S.; Maag, D.; Arnold, J.J.; Zhong, W.; Lau, J.Y.N.; Andino, R.; Cameron, C.E. The broad-spectrum antiviral ribonucleoside ribavirin is an RNA virus mutagen. *Nat. Med.* **2000**, *6*, 1375–1379. [CrossRef]
41. Toledo-Ibelles, P.; Gutiérrez-Vidal, R.; Calixto-Tlacomulco, S.; Delgado-Coello, B.; Mas-Oliva, J. Hepatic Accumulation of Hypoxanthine: A Link Between Hyperuricemia and Nonalcoholic Fatty Liver Disease. *Arch. Med. Res.* **2021**, *52*, 692–702. [CrossRef] [PubMed]
42. Brasili, E.; Mengheri, E.; Tomassini, A.; Capuani, G.; Roselli, M.; Finamore, A.; Sciubba, F.; Marini, F.; Miccheli, A. Lactobacillus acidophilus La5 and Bifidobacterium lactis Bb12 Induce Different Age-Related Metabolic Profiles Revealed by 1H-NMR Spectroscopy in Urine and Feces of Mice. *J. Nutr.* **2013**, *143*, 1549–1557. [CrossRef] [PubMed]